

# Synthesis and Characterization of Thermally Crosslinkable Hole-Transporting Polymers for PLEDs

Sang-Mi Park,<sup>1</sup> Kyoung-Soo Yook,<sup>2</sup> Woo-Hyung Lee,<sup>1</sup> Yongtaek Hong,<sup>3</sup> Jun-Yeob Lee,<sup>2</sup> In-Nam Kang<sup>1</sup>

<sup>1</sup>Department of Chemistry, The Catholic University of Korea, Bucheon, Gyeonggi-do 420–743, Korea

<sup>2</sup>Department of Polymer Science and Engineering, Dankook University, Jukjeon-dong, Yongin, Korea

<sup>3</sup>Department of Electrical Engineering and Computer Science, Seoul National University, Seoul 151–744, Korea

Correspondence to: I.-N. Kang (E-mail: inamkang@catholic.ac.kr) or J.-Y. Lee (E-mail: lee17@dankook.ac.kr)

Received 22 July 2013; accepted 7 September 2013; published online 25 September 2013

DOI: 10.1002/pola.26943

**ABSTRACT:** Two new thermally crosslinkable hole-transporting polymers, X-PTPA and X-PCz, were synthesized via Yamamoto coupling reactions. The number-averaged molecular weights ( $M_n$ ) of X-PTPA and X-PCz were found to be 45,000 and 48,000, respectively, and therewith, polydispersity indices were of 1.8 and 1.7, respectively. Thermally crosslinked X-PTPA and X-PCz exhibit excellent solvent resistance and stable optoelectronic properties. The UV–visible maximum absorption peaks of X-PTPA and X-PCz in the thin film state are at 389 and 322 nm, respectively. The HOMO levels of X-PTPA and X-PCz are estimated to be  $-5.27$  and  $-5.39$  eV, respectively. Multilayered devices (ITO/crosslinked X-PTPA or X-PCz/SY-PPV/LiF/Al) were fabricated with SY (SuperYellow) as the emitting layer. The

maximum efficiency of the multilayered device with a crosslinked X-PTPA layer is approximately three times higher than that of the device without a crosslinked X-PTPA layer and much higher than that of the crosslinked X-PCz device. This result can be explained by the observations that crosslinked X-PTPA produces increased electron accumulation within the emitter, SY, and also efficient exciton formation due to improved charge balance. © 2013 Wiley Periodicals, Inc. *J. Polym. Sci., Part A: Polym. Chem.* **2013**, *51*, 5111–5117

**KEYWORDS:** charge transport; conjugated polymers; functionalization of polymers; heteroatom-containing polymers; light-emitting diodes (LED)

**INTRODUCTION** Solution-processed polymer light-emitting diodes (PLEDs) have great promise because of their potential applications in large-area flat panel displays and solid-state lighting.<sup>1–3</sup> However, single-layer PLEDs usually exhibit limited device performance because of unbalanced transport and injection of charge carriers. To address these problems, a multilayer device is usually fabricated by inserting an interlayer such as a hole-transporting layer (HTL) or an electron-transporting layer.<sup>4–6</sup> The incorporation of interlayer polymers with thicknesses of 10–30 nm on top of the PEDOT:PSS layer has previously been reported to improve PLED device performance. For example, the incorporation of a poly(9,9-dioctylfluorene-*co-N*-(4-butylphenyl)-diphenylamine) interlayer (10 nm) on top of the PEDOT:PSS layer was shown to improve the efficiency and lifetime of the PLED device.<sup>7</sup> This improved performance was explained as due to the exciton-blocking effects of the interlayer, which prevent luminescence quenching. However, in most cases, such interlayer materials are affected by the subsequent solution processing of the emitting layer (EML). Thus, the

development of insoluble interlayer materials has become an important issue for the implementation of solution-processed multilayer PLEDs. Several methods for overcoming the issues associated with the solution processing of multilayer structures have been tested.<sup>8–12</sup> One fascinating approach is the combination of crosslinkable polymers and small molecules in the hole-transport layer, which can be solution processed by spin casting and then transformed into an insoluble film with light or thermal treatment.<sup>13–19</sup>

In this article, we describe two new thermally crosslinkable hole-transporting polymers, X-PTPA and X-PCz, for use in solution processable multilayer PLEDs. These polymers contain thermally crosslinkable dibutenylfluorene groups as well as hole-transporting triphenylamine or carbazole units. The syntheses and characterizations of these polymers are presented. The solution-processable multilayer PLEDs containing crosslinked X-PTPA and X-PCz exhibit device performances that are significantly better than those of single hole-transport layer PLEDs.

Additional Supporting Information may be found in the online version of this article.

© 2013 Wiley Periodicals, Inc.

## EXPERIMENTAL

### Instrumentations

$^1\text{H}$  and  $^{13}\text{C}$  NMR spectra were recorded on Bruker AVANCE 300 spectrometer, with tetramethylsilane as an internal reference. Elemental analysis was done by using PerkinElmer 2400 Series II CHNS/O Analyzer. The optical absorption spectra were measured by a Shimadzu UV-3100 UV-vis-NIR spectrometer. The number- and weight-average molecular weights of polymers were determined by gel permeation chromatography (GPC) on Viscotek T60A instrument, using chloroform as eluent and polystyrene as standard. The differential scanning calorimetry (DSC) was measured by using a TA Q100 instrument and operated under nitrogen atmosphere. Cyclic voltammetry (CV) was performed on an AUTO-LAB/PG-STAT12 model system with a three-electrode cell in a solution of  $\text{Bu}_4\text{NBF}_4$  (0.10 M) in acetonitrile at a scan rate of  $50 \text{ mV s}^{-1}$ . Polymer film coatings on ITO anode electrode were formed by spin-coating method.

### Fabrication of the Polymer OLEDs

A device structure of indium tin oxide (ITO, 150 nm)/polyethylene-3,4-dioxythiophene:polystyrene-sulfonate (PEDOT:PSS, 60 nm)/X-PTPA or X-PCz (20 nm)/SY (50 nm)/LiF/Al was used. SY (SuperYellow) from Merck was a yellow emitting material. Current density–voltage–luminance and electroluminescence (EL) characteristics of the devices were obtained by Keithley 2400 source measurement unit and a Minolta CS 1000 spectroradiometer.

### Fabrication of the Organic Thin-Film Transistors

Organic thin-film transistor (OTFT) devices were fabricated in a bottom-contact geometry (channel length =  $12 \mu\text{m}$ , width =  $120 \mu\text{m}$ ). The source and drain contacts consisted of gold (100 nm), and the dielectric was silicon oxide ( $\text{SiO}_2$ ) with a thickness of 300 nm. The  $\text{SiO}_2$  surface was cleaned, dried, and pretreated with a solution of 1.0 mM octyltrichlorosilane in toluene at room temperature for 2 h under nitrogen to produce nonpolar and smooth surfaces onto which the polymers could be spin-coated. The polymers were dissolved to a concentration of 0.5 wt % in chlorobenzene. Films of the organic semiconductors were spin-coated at 1500 rpm for 50 s to a thickness of 50 nm, followed by thermal treatment at  $230 \text{ }^\circ\text{C}$  for 30 min under nitrogen atmosphere. The field effect mobility was calculated in the saturation regime by using the equation  $I_{\text{DS}} = (\mu WC_i/2L)(V_G - V_T)^2$ , where  $I_{\text{DS}}$  is the drain-source current,  $\mu$  is the field effect mobility,  $W$  is the channel width,  $L$  is the channel length,  $C_i$  is the capacitance per unit area of the gate dielectric layer, and  $V_G$  is the gate voltage.

### Materials

1-Bromo-4-(octyloxy)benzene (**1**)<sup>20</sup> and 3,6-dibromo-9-octyl-9H-carbazole (**5**)<sup>21</sup> were synthesized according to previously published procedures.

### 4-(Octyloxy)-N,N-diphenylbenzenamine (2)

Compound **1** (3 g, 10.52 mmol), diphenylamine (1.87 g, 11.05 mmol), sodium tert-butoxide (3.03 g, 31.53 mmol),

$\text{Pd}_2(\text{dba})_3$  [tris(dibenzylidene acetone)dipalladium(0)] (0.48 g, 0.52 mmol), and tricyclohexyl phosphine (0.21 g, 0.75 mmol) were dissolved in 200 mL of toluene and kept under nitrogen at  $120 \text{ }^\circ\text{C}$  for 5 h. When the reaction had finished, the reaction mixture was cooled to room temperature, quenched by addition of 200 mL of water, and then extracted three times using chloroform and water. The organic layer was separated and dried with anhydrous magnesium sulfate, and then the solvent was removed using a rotary evaporator. The crude product was purified by column chromatography using a cosolvent (toluene:hexane = 1:2 [v/v]) as the eluting solvent. The product yield was 77% (3.03 g).

$^1\text{H}$  NMR ( $\text{CDCl}_3$ , 300 MHz,  $\delta$ ) 7.17–7.23 (m, 4H), 7.01–7.06 (m, 6H), 6.91–6.95 (m, 2H), 6.81–6.84 (m, 2H) 3.93 (t, 2H), 1.75 (m, 2H), 1.29–1.48 (m, 10H), 0.89 (t, 3H).  $^{13}\text{C}$  NMR ( $\text{CDCl}_3$ , 75 MHz,  $\delta$ ) 156.05, 148.46, 140.80, 129.25, 127.55, 123.08, 121.99, 115.60, 68.52, 32.04, 29.59, 29.45, 26.31, 22.87, 14.28. Anal. Calcd. for  $\text{C}_{26}\text{H}_{31}\text{NO}$ : C, 83.6; H, 8.37; N, 3.75; O, 4.28. Found: C, 83.51; H, 8.34; N, 3.79; O, 4.30.

### 4-Bromo-N-(4-bromophenyl)-N-(4-(octyloxy)-phenyl)benzenamine (3)

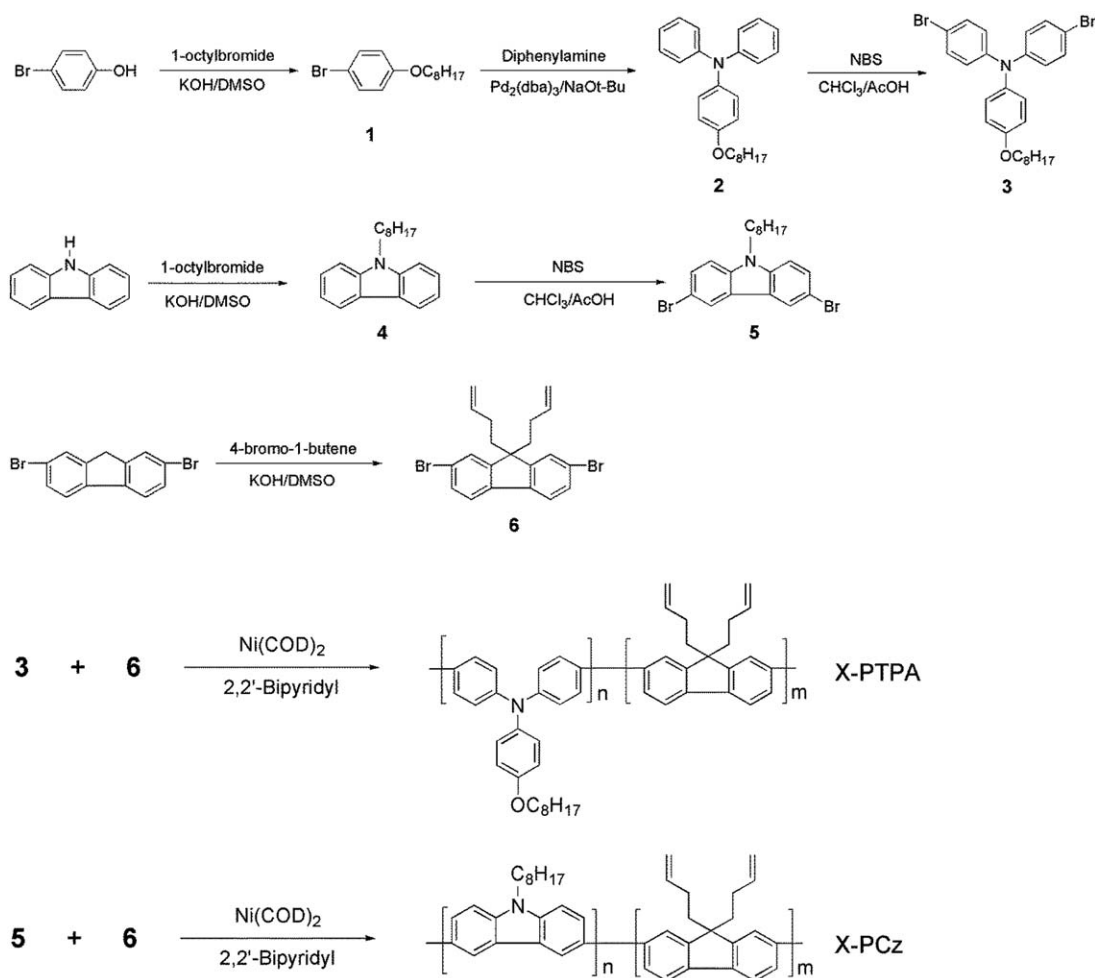
Compound **2** (3 g, 8.10 mmol) was dissolved in 20 mL of chloroform and 40 mL of acetic acid, and then *N*-bromosuccinimide (2.91 g, 16.35 mmol) was added and the solution was stirred for 2 h at  $0 \text{ }^\circ\text{C}$ . Dilute aqueous sodium hydroxide was then added and the reaction mixture was stirred for a further 30 min. The reaction mixture was extracted three times using chloroform and brine; the organic layer was separated and dried with anhydrous magnesium sulfate, and then the solvent was removed using a rotary evaporator. The crude product was purified by column chromatography using a cosolvent (toluene:hexane = 1:10 [v/v]) as the eluting solvent. The product yield was 69% (2.95 g).

$^1\text{H}$  NMR ( $\text{CDCl}_3$ , 300 MHz,  $\delta$ ) 7.26–7.80 (m, 4H), 6.99–7.03 (m, 2H), 6.81–6.91 (m, 6H), 3.93 (t, 2H), 1.82 (m, 2H), 1.29–1.48 (m, 10H), 0.89 (t, 3H).  $^{13}\text{C}$  NMR ( $\text{CDCl}_3$ , 75 MHz,  $\delta$ ) 156.60, 147.07, 139.70, 132.36, 127.65, 124.45, 115.80, 114.69, 68.52, 32.04, 29.58, 29.53, 29.46, 26.29, 22.88, 14.31. Anal. Calcd. for  $\text{C}_{26}\text{H}_{29}\text{Br}_2\text{NO}$ : C, 58.77; H, 5.50; N, 2.64; O, 3.01. Found: C, 58.78; H, 5.49; N, 2.69; O, 3.16.

### 2,7-Dibromo-9,9-di(but-3-enyl)-9H-fluorene (6)

2,7-Dibromo-9H-fluorene (1 g, 3.09 mmol), KOH (0.38 g, 6.77 mmol), and 4-bromo-1-butene (0.81 mL, 6.00 mmol) were dissolved in 15 mL of dimethylsulfoxide (DMSO). The resulting mixture was stirred at room temperature for 5 h, and then poured into 200 mL water. The organic phase was extracted with chloroform (100 mL  $\times$  3). The organic layer was separated and dried with anhydrous magnesium sulfate, and then the solvent was removed using a rotary evaporator. The crude product was purified by silica gel chromatography using *n*-hexane as the eluent. The product yield was 78% (1.03 g, white solid).

$^1\text{H}$  NMR ( $\text{CDCl}_3$ , 300 MHz,  $\delta$ ) 7.50–7.53 (m, 2H), 7.44–7.47 (m, 4H), 5.48–5.62 (m, 2H), 4.74–4.80 (m, 4H), 2.03–2.09



**SCHEME 1** Synthetic routes for the monomers and polymer.

(m, 4H), 1.31–1.39 (m, 4H)  $^{13}\text{C}$  NMR ( $\text{CDCl}_3$ , 75 MHz,  $\delta$ ) 151.50, 139.20, 138.01, 130.59, 126.26, 121.73, 121.28, 114.42, 55.22, 39.22, 27.98. Anal. Calcd. for  $\text{C}_{21}\text{H}_{20}\text{Br}_2$ : C, 58.36; H, 4.66 Found: C, 58.32; H, 4.69.

#### X-PTPA

Compound **3** (0.403 g, 0.76 mmol), compound **6** (36 mg, 0.083 mmol), 2,2'-bipyridyl (0.26 g, 1.66mmol), and bis(1,5-cyclooctadiene)nickel(0) (0.46 g, 1.67 mmol) were dissolved in 15 mL of anhydrous THF under nitrogen. The mixture was stirred for 24 h at 60 °C. When the reaction had finished, the reaction mixture was precipitated from the 10 mL of HCl and 150 mL of methanol. The polymer was dissolved in small amount of toluene and precipitated in methanol. The resulting polymer was purified through Soxhlet extraction using acetone and methanol. The polymer, X-PTPA, was a light yellow solid (0.24 g).

$^1\text{H}$  NMR ( $\text{CDCl}_3$ , 300 MHz,  $\delta$ ) 7.41–7.55 (m, 4H), 7.11 (s, 5H), 6.87 (s, 2H), 5.54–5.63 (m, 2H), 4.75–4.80 (m, 4H), 3.95 (s, 2H), 2.17 (s, 4H) 1.75–1.80 (m, 2H), 1.29–1.46 (m, 10H), 0.89 (m, 3H). ELEM. ANAL.: C, 84.96; H, 7.73; N, 3.18; O, 4.19.

#### X-PCz

Compound **5** (0.332 g, 0.76 mmol), compound **6** (36 mg, 0.083 mmol), 2,2'-bipyridyl (0.26 g, 1.66mmol), and bis(1,5-cyclooctadiene)nickel(0) (0.46 g, 1.67 mmol) were dissolved in 15 mL of anhydrous THF under nitrogen. The mixture was stirred for 24 h at 60 °C. When the reaction had finished, the reaction mixture was precipitated from the 10 mL of HCl and 150 mL of methanol. The polymer was dissolved in small amount of toluene and precipitated in methanol. The resulting polymer was purified through Soxhlet extraction using acetone and methanol. The polymer, X-PCz, was a white-yellowish solid (0.15 g).

$^1\text{H}$  NMR ( $\text{CDCl}_3$ , 300 MHz,  $\delta$ ) 8.48–8.53 (d, 2H), 7.74–7.87 (m, 4H), 7.50 (s, 2H), 5.63–5.65 (s, 2H), 4.79–4.86 (d, 4H), 4.37 (s, 2H), 2.27 (s, 4H), 1.93 (s, 2H), 1.25 (m, 10H), 0.85 (m, 3H). ELEM. ANAL.: C, 87.5; H, 8.39; N, 4.25.

## RESULTS AND DISCUSSION

### Synthesis and Characterization of the Polymers

The synthetic routes for the monomers and polymers are outlined in Scheme 1. The crosslinkable polymers, X-PTPA

**TABLE 1** Physical Properties of X-PTPA and X-PCz

Polymer	Feed Ratio ( <i>n:m</i> )	Actual Ratio ( <i>n:m</i> )	$M_n$ (kDa)	$M_w$ (kDa)	PDI
X-PTPA	90:10	90.4:9.6	45	81	1.8
X-PCz	90:10	90.9:9.1	48	84	1.7

and X-PCz, were prepared via Ni(0)-mediated Yamamoto polymerizations. These polymers are soluble in common organic solvents, such as tetrahydrofuran (THF), chloroform, and toluene, without any evidence of gel formation at room temperature. The molecular weights and polydispersity indices of the polymers were determined by performing GPC with THF as the eluent and polystyrene as the standard. The number-averaged molecular weights of X-PTPA and X-PCz were found to be 45,000 and 48,000 with polydispersity indices of 1.8 and 1.7, respectively. The actual ratios of the monomers within the polymers were determined by using  $^1\text{H}$  NMR spectroscopy (see Supporting Information Fig. S1). From the  $^1\text{H}$  NMR spectrum of the X-PTPA, a triplet peak at  $\delta = 3.94$  and a multiplet signal at  $\delta = 5.58$  were observed, which were assigned to the methyl protons on the triphenylamine unit and the vinyl protons on the fluorene unit, respectively. The actual composition of the X-PTPA was determined by integrating of those two signals. In the case of the X-PCz, two signals at  $\delta = 4.30$  and  $5.63$  were used to determine the actual composition. The physical properties of the polymers are summarized in Table 1.

### Thermal Properties and Crosslinking Conditions of the Polymers

Thermal gravimetric analysis (TGA) and DSC was used to investigate the thermal and crosslinking properties of the polymers (Fig. 1 and Supporting Information Fig. S2). The broad exothermic peaks between 200 and 260 °C in the first scan are due to the thermal crosslinking of the butenyl groups. No exothermic peaks are evident during the second heating cycle of the polymers, which indicates that the crosslinking reactions are completed during the first heating cycle. The thermograms for X-PTPA and X-PCz contained a broad glass transition temperature ( $T_g$ ) at 125 and 182 °C, respectively, in the first heating scan. On the second heating, the  $T_g$  of the crosslinked X-PTPA and X-PCz was slightly raised to 130 and 190 °C, respectively. None of the polymers exhibited melting or crystalline transition behaviors, which suggested that the polymers assumed amorphous structures. On the basis of these DSC results, we employed isothermal heating at 230 °C for 30 min under a nitrogen atmosphere to ensure complete crosslinking. The excellent thermal stabilities of the X-PTPA and X-PCz are evident from their TGA profiles, which displayed decomposition temperatures above 400 °C.

### Optical and Electrochemical Properties and Solvent Resistance

The UV-visible absorption and PL emission spectra of X-PTPA and X-PCz in the film state are shown in Figure 2.

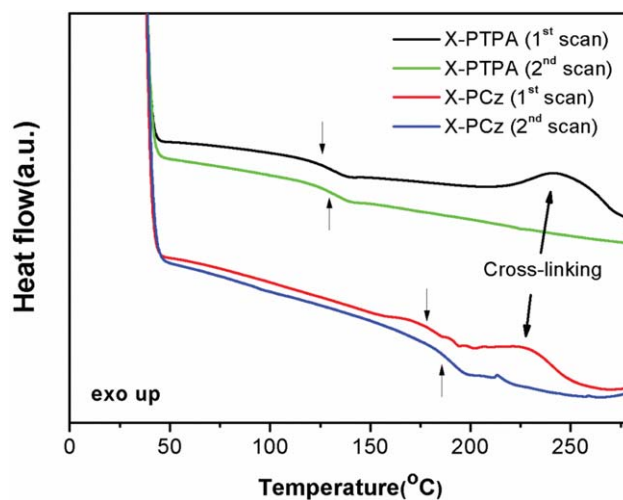


**FIGURE 1** DSC thermograms of X-PTPA and X-PCz for a heating rate of 5 °C min<sup>-1</sup> under an inert atmosphere. [Color figure can be viewed in the online issue, which is available at [wileyonlinelibrary.com](http://wileyonlinelibrary.com).]

These spectra are structureless, which indicates that the polymers are in amorphous morphological states. The absorption maxima ( $\lambda_{\text{max}}$ ) of X-PTPA and X-PCz are at 388 and 322 nm, respectively, and are ascribed to the  $\pi-\pi^*$  transitions of the conjugated polymer backbone. The absorption spectra of the polymer thin films before and after crosslinking are identical, which indicates that the crosslinking reactions of the butenyl side groups in the polymers produce network structures without any decomposition of the polymer backbones. According to the cut-off absorption edge wavelengths, the optical band gap energies of X-PTPA and X-PCz are 2.85 and 3.0 eV, respectively.

The photoluminescence (PL) maxima of the pristine X-PTPA and X-PCz films are at 449 and 425 nm, respectively. The PL

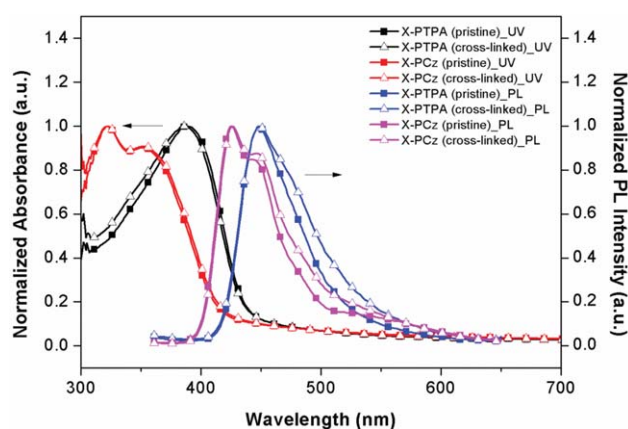


**FIGURE 2** UV-visible absorption and PL emission spectra of X-PTPA and X-PCz before and after crosslinking. [Color figure can be viewed in the online issue, which is available at [wileyonlinelibrary.com](http://wileyonlinelibrary.com).]

**TABLE 2** Electrochemical Properties of the Pristine and Cross-linked HTL Polymers

	X-PTPA		X-PCz	
	Pristine	Crosslinked	Pristine	Crosslinked
UV <sub>max</sub> (nm)	389	385	322	323
PL <sub>max</sub> (nm)	448	449	425	426
E <sub>g</sub> <sup>opt</sup> (eV)	2.85	2.85	3.00	3.00
HOMO (eV)	-5.27	-5.27	-5.39	-5.39
LUMO (eV)	-2.42	-2.42	-2.39	-2.39

shoulder peaks of the polymer thin films are located in the longer wavelength region and broaden slightly after cross-linking reaction, whereas the emission maxima of the polymers in the shorter wavelength region remain almost unchanged. PL broadening of the polymer thin films may be due to keto effect of the fluorene units.<sup>22</sup> The optical and photoluminescence properties of the polymers are summarized in Table 2. The solvent resistances of the crosslinked polymers were investigated by comparing the UV-visible spectra of each crosslinked polymer film before and after rinsing with toluene, which is a good solvent for the film (see Supporting Information Fig. S3). The X-PTPA and X-PCz films were spin-coated from toluene solution onto an ITO substrate and then thermally crosslinked in a nitrogen-filled glove box. After curing at 230 °C for 30 min, we dropped toluene onto each crosslinked polymer film and spun the whole substrate. The variation in the absorption spectrum of the crosslinked X-PTPA film is negligible after rinsing with toluene; the absorption intensity of the film is ~95% of its initial value after rinsing, which indicates that crosslinked X-PTPA is highly solvent resistant after thermal crosslinking. When the X-PTPA film was rinsed with toluene solvent before thermal crosslinking, the absorption intensity of the film drastically decreased because of the removing of the polymer during the toluene washing process, which indicates that the crosslinking condition is proper in the X-PTPA [Supporting Information Fig. S3(c)]. In the case of the X-PCz film, the crosslinked X-PCz film is slightly affected by toluene: the absorption intensity of the film is approximately 85% of its initial value after rinsing. The difference of solvent resistance of two polymers may be due to the difference of actual composition of crosslinking monomer units. These results show that the synthesized polymers are suitable for the fabrication of solution-processed multilayer PLEDs.

The highest occupied molecular orbital (HOMO) levels of the polymer films were calculated from the CV results by using the equation  $E_{\text{HOMO}} = -(E_{\text{ox}} + 4.8)$  eV, where  $E_{\text{ox}}$  is the onset oxidation potential relative to the ferrocene external standard (Supporting Information Fig. S4). The HOMO levels of the pristine X-PTPA and X-PCz films were estimated to be -5.27 and -5.39 eV, respectively, and the HOMO values before and after crosslinking are identical. The optical band gaps of X-PTPA and X-PCz were determined from the onset of absorption and found to be 2.85 and 3.0 eV, respectively.

The lowest unoccupied molecular orbital (LUMO) levels of the X-PTPA and X-PCz films were calculated to be -2.42 and -2.39 eV, respectively.

### Electroluminescence Properties of Multilayer PLEDs Using Crosslinked X-PTPA and X-PCz

To evaluate the hole-transport properties of X-PTPA and X-PCz layers in multilayer devices, PLEDs [ITO/PEDOT:PSS/ X-PTPA or X-PCz/SY/LiF(5 nm)/Al(100 nm)] were fabricated by using successive spin-coating processes. X-PTPA and X-PCz were spin-coated on top of the PEDOT:PSS layers and treated at 230 °C for 30 min under a nitrogen atmosphere, followed by the spin-coating of SY (SuperYellow) solution. To evaluate the device characteristics, we prepared a series of solution-processed PLED devices as follows:

- 1) Device A: ITO/PEDOT:PSS (60 nm)/SY (40 nm)/LiF/Al
- 2) Device B: ITO/PEDOT:PSS (60 nm)/X-PTPA (20 nm) /SY (40 nm)/LiF/Al
- 3) Device C: ITO/PEDOT:PSS (60 nm)/X-PCz (20 nm)/SY (40 nm)/LiF/Al

The EL spectra of devices A, B, and C are shown in Figure 3. Devices A, B, and C have yellow emission spectra with a maximum emission peak at 548 nm and a shoulder at 588 nm, which correspond to the PL emission peaks of the SY emitting polymer (see Supporting Information Fig. S5), so the EL emissions of the devices are due to the SY EML not the X-PTPA or X-PCz layers. The current density–voltage ( $I$ – $V$ ), brightness–voltage ( $L$ – $V$ ), and efficiency–brightness characteristics of devices A, B, and C are shown in Figures 4 and 5, respectively, and representative results are summarized in Table 3. The turn-on voltages ( $V_{\text{on}}$ ) for the devices are in the range 2.5–3.0 V. A low turn-on voltage was observed even if crosslinked X-PTA or X-PCz are inserted between the PEDOT:PSS layer and the EML. When the devices with X-PTPA and X-PCz as the HTL (devices B and C) are compared, it is evident that device B exhibits higher performance: it has a higher maximum current efficiency (4.22 cd A<sup>-1</sup> at 5.0

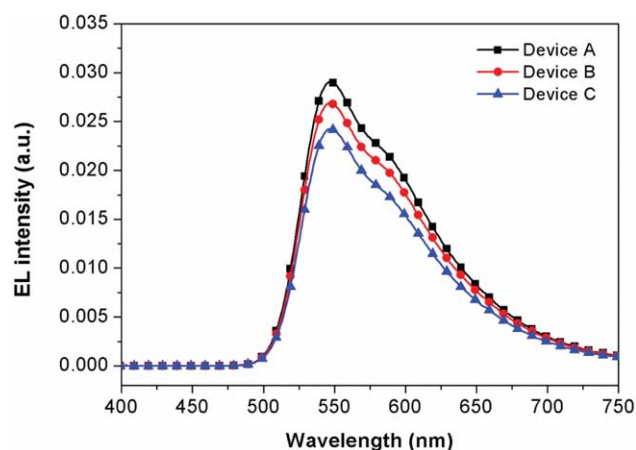


**FIGURE 3** EL spectra of devices A, B, and C. [Color figure can be viewed in the online issue, which is available at [wileyonlinelibrary.com](http://www.intelibrary.com).]

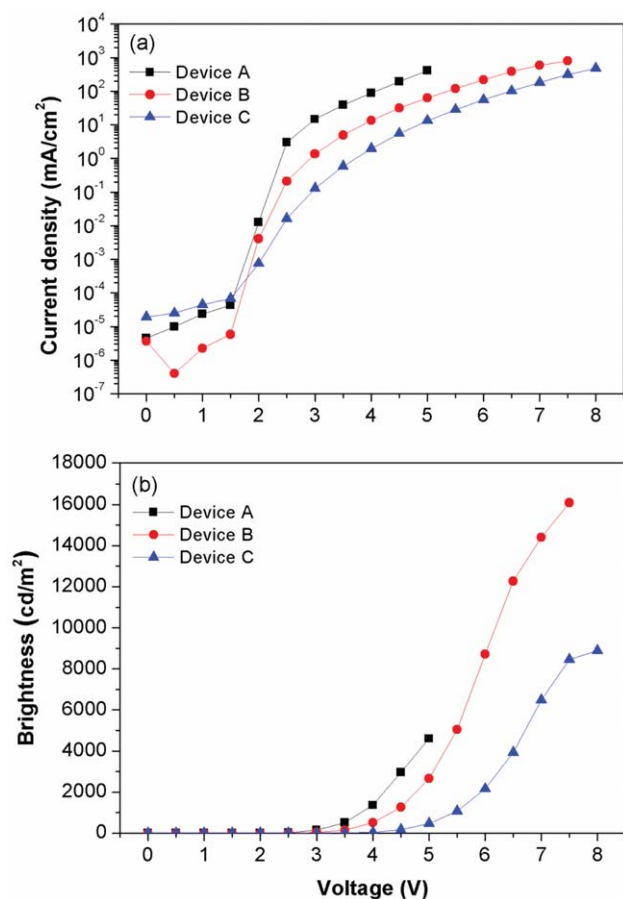


**FIGURE 4** (a) *I*-*V* and (b) *V*-*L* characteristics of devices A, B, and C. [Color figure can be viewed in the online issue, which is available at [wileyonlinelibrary.com](http://wileyonlinelibrary.com).]

V) and a higher maximum brightness (16,000 cd m<sup>-2</sup> at 7.5 V). The differences between the performances of devices B and C are presumably due to the difference between the HOMO energy levels of X-PTA and X-PCz. The work function of PEDOT:PSS and the HOMO level of SY are -5.0 and -5.3 eV, respectively.<sup>23</sup> These results suggest that X-PTPA (its HOMO level is at -5.27 eV) is a more suitable energy intermediate than X-PCz (-5.39 eV) in that it provides a better cascade hole-transporting pathway and enables a better balance of charge carriers. The lower HOMO level of X-PCz also means that the energy barrier at the PEDOT/X-PCz interface is higher, which results in unbalanced charge transportation and lower device performance.

Another reason for the superior performance of device B is that X-PTPA has higher hole mobility than X-PCz. To determine the hole mobilities of the crosslinked HTL polymers, thin-film transistors were fabricated with the two polymers after thermal treatment. The transfer characteristics of the crosslinked X-PTPA and X-PCz TFT devices are shown in Supporting Information Figure S6. The saturation hole mobilities of X-PTPA and X-PCz were found to be  $1.0 \times 10^{-4}$  and  $5.0 \times 10^{-6}$  cm<sup>2</sup>V<sup>-1</sup>s<sup>-1</sup>, respectively. The hole mobility of crosslinked X-PTPA is 20 times higher than that of cross-

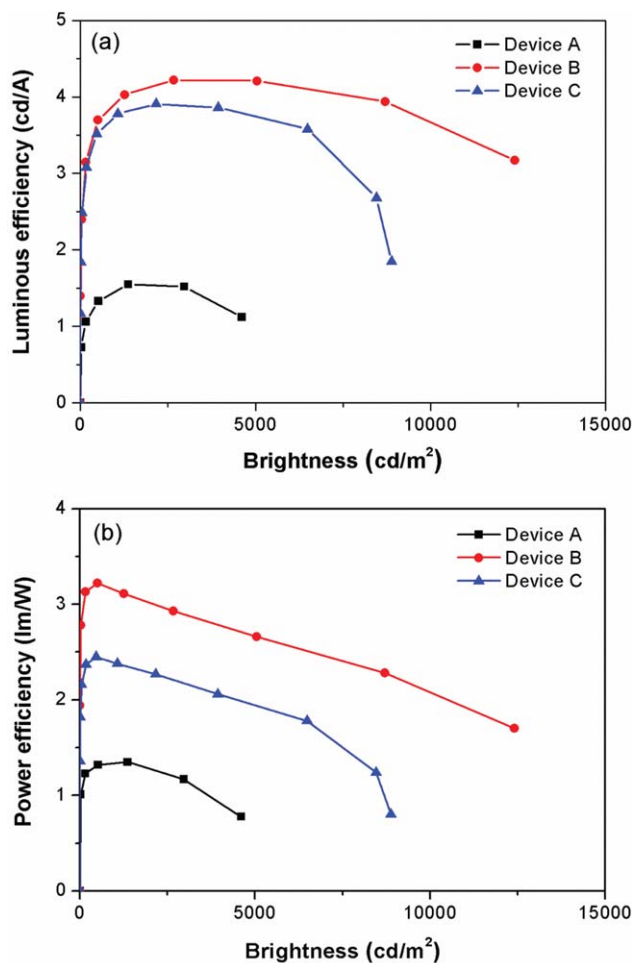


**FIGURE 5** (a) Current efficiency-brightness and (b) power efficiency-brightness characteristics of devices A, B, and C. [Color figure can be viewed in the online issue, which is available at [wileyonlinelibrary.com](http://wileyonlinelibrary.com).]

linked X-PCz. Thus the superior performance of device B is due to its cascade hole injection and fast hole transportation. It should be noted that the devices incorporating these crosslinked HTL polymers exhibit much better performance than the control device (ITO/PEDOT:PSS/SY/LiF/Al). The maximum luminescence efficiency of the device with X-PTPA is approximately three times higher than that of the control device (device A).

This pronounced improvement in device performance is due to the balanced charge injection and transport

**TABLE 3** Electroluminescence Data for Devices A, B, and C

Devices	$V_{on}$ (V) <sup>a</sup>	$L_{max}$ (cd m <sup>-2</sup> )	$LE_{max}$ (lm W <sup>-1</sup> )	$LE_{max}$ (cd A <sup>-1</sup> )
A	2.5	4,600	1.35	1.55
B	2.5	16,000	3.22	4.22
C	3.0	8,900	2.45	3.91

<sup>a</sup> Turn-on voltage ( $V_{on}$ ): voltage at a luminance of 10 cd m<sup>-2</sup>.

characteristics, which lead to effective charge recombination within the SY EML.

## CONCLUSIONS

We have demonstrated a facile and simple method for the synthesis of the thermally crosslinkable hole-transporting polymers, X-PTPA and X-PCz. The polymers are composed of thermally crosslinkable dibutenylfluorene groups as well as hole-transporting triphenylamine or carbazole units. After thermal crosslinking at 230 °C for 30 min, crosslinked X-PTPA and X-PCz exhibit excellent solvent resistance. Furthermore, the optical and electrochemical properties of the synthesized HTL polymers do not change after thermal crosslinking. Multi-layer PLEDs using these crosslinked HTL polymers were successfully fabricated by using successive spin-coating processes. The insertion of thermally crosslinked X-PTPA and X-PCz as HTLs was found to significantly improve device performance. The maximum brightness and maximum luminance efficiency of the PLED using X-PTPA were found to be 16,000 cd m<sup>-2</sup> and 4.22 cd A<sup>-1</sup>, respectively, with an efficiency that is approximately three times higher than that of the device without an X-PTPA layer (1.55 cd A<sup>-1</sup>).

## ACKNOWLEDGMENTS

This research was supported by the Industrial Strategic Technology Development Program (KI002104, Development of Fundamental Technologies for Flexible Combined-Function Organic Electronic Device) funded by the Ministry of Knowledge Economy (MKE, Korea).

## REFERENCES AND NOTES

- 1 J. H. Burroughes, D. D. C. Bradley, A. R. Brown, R. N. Marks, K. Mackay, R. H. Friend, P. L. Burns, A. B. Holmes, *Nature* **1990**, *347*, 539–541.
- 2 R. H. Friend, R. W. Gymer, A. B. Holmes, J. H. Burroughes, R. N. Marks, C. Taliani, D. D. C. Bradley, D. A. D. Santos, J. L. Bredas, M. Logdlund, W. R. Salaneck, *Nature* **1999**, *397*, 121–128.
- 3 B. W. D'Andrade, S. R. Forrest, *Adv. Mater.* **2004**, *16*, 1585–1595.
- 4 F. Huang, Y.-J. Cheng, Y. Zhang, M. S. Liu, A. K.-Y. Jen, *J. Mater. Chem.* **2008**, *18*, 4495–4509.
- 5 A. P. Kulkarni, C. J. Tonzola, A. Babel, S. A. Jenekhe, *Chem. Mater.* **2004**, *16*, 4556–4573.
- 6 Z. Jiang, W. Zhang, H. Yao, C. Yang, Y. Cao, J. Qin, G. Yu, Y. Liu, *J. Polym. Sci. Part A: Polym. Chem.* **2009**, *47*, 3651–3661.
- 7 J.-S. Kim, R. H. Friend, I. Grizzi, J. H. Burroughes, *Appl. Phys. Lett.* **2005**, *87*, 023506–023508.
- 8 E. Bacher, M. Bayerl, P. Rudati, N. Reckefuss, C. D. Muller, K. Meerholz, O. Nuyken, *Macromolecules* **2005**, *38*, 1640–1647.
- 9 Y.-H. Niu, M. S. Liu, J.-W. Ka, J. Bardeker, M. T. Zin, R. Schofield, Y. Chi, A. K.-Y. Jen, *Adv. Mater.* **2007**, *19*, 300–304.
- 10 M. J. Harding, D. Poplavskyy, V.-E. Choong, A. J. Campbell, F. So, *Org. Electron.* **2008**, *9*, 183–190.
- 11 X. Z. Jiang, S. Liu, M. S. Liu, P. Herguth, A. K.-Y. Jen, H. Fong, M. Sarikaya, *Adv. Funct. Mater.* **2002**, *12*, 745–751.
- 12 K. Zhu, S. T. Iacono, S. M. Budy, J. Jin, D. W. Smith, *J. Polym. Sci. Part A: Polym. Chem.* **2010**, *48*, 1887–1893.
- 13 Y.-J. Cheng, M.-H. Liao, H.-M. Shih, P.-I. Shih, C.-S. Hsu, *Macromolecules* **2011**, *44*, 5968–5976.
- 14 W.-F. Su, Y. Chen, *Polymer* **2011**, *52*, 77–85.
- 15 W.-F. Su, R.-T. Chen, Y. Chen, *J. Polym. Sci. Part A: Polym. Chem.* **2011**, *49*, 352–360.
- 16 B. Ma, B. J. Kim, D. A. Poulsen, S. J. Pastine, J. M. J. Frechet, *Adv. Funct. Mater.* **2009**, *19*, 1024–1031.
- 17 A. R. Davis, J. A. Maegerlein, K. R. Carter, *J. Am. Chem. Soc.* **2011**, *133*, 20546–20551.
- 18 F. B. Koyuncu, A. R. Davis, K. R. Carter, *Chem. Mater.* **2012**, *24*, 4410–4416.
- 19 J. R. Cox, H. A. Kang, T. Igarashi, T. M. Swager, *ACS Macro Lett.* **2012**, *1*, 334–337.
- 20 W. G. George, H. Michael, L. David, J. T. Kenneth, *J. Chem. Soc. Perkin Trans. 2* **1989**, *12*, 2041–2053.
- 21 K. Brunner, A. Dijken, H. Börner, J. J. A. M. Bastiaansen, N. M. M. Kiggen, B. M. W. Langeveld, *J. Am. Chem. Soc.* **2004**, *126*, 6035–6042.
- 22 Y.-S. Wu, J. Li, X.-C. Ai, L.-M. Fu, J.-P. Zhang, Y.-Q. Fu, J.-J. Zhou, L. Li, Z.-S. Bo, *J. Phys. Chem. A* **2007**, *111*, 11473–11479.
- 23 H. Becker, H. Spretizer, W. Kreuder, E. Kluge, H. Schenk, I. Parker, Y. Cao, *Adv. Mater.* **2000**, *12*, 42–48.